

# EVALUATION OF THE USE OF A SEMI-HYPERBOLIC DIE FOR MEASURING ELONGATIONAL VISCOSITY OF POLYMER MELTS

DONALD G. BAIRD\*, TUNG W. CHAN, CHRISTOPHER MCGRADY, SYED M. MAZAHIR

Department of Chemical Engineering, Virginia Polytechnic Institute and State University,  
Blacksburg, VA 24061, USA

\* Email: [dbaird@vt.edu](mailto:dbaird@vt.edu)

Fax: x1.540.231.2732

Received: 2.9.2009, Final version: 15.10.2009

## ABSTRACT:

The semi-hyperbolic (SHPB) die with and possibly without wall lubrication has been proposed as a device for measuring the elongational viscosity of polymeric fluids. Using numerical simulation under the condition of complete wall slip, it was found for two polyethylenes (LDPE and LLDPE) that the calculated elongational viscosity values agreed well with strain-averaged values,  $\langle\eta_e\rangle$ , obtained from independent measurements in stretching type rheometers. This is in agreement with the original hypothesis of Everage and Ballman (E-B). Numerical simulations showed that the Baird and Huang (B-H) approach for calculating  $\langle\eta_e\rangle$ , which accounts for the shear stress due to geometric considerations in the presence of complete slip, agreed with data better than did the E-B approach. Numerical simulations using varying degrees of wall slip indicated that reasonable values of  $\langle\eta_e\rangle$  could be obtained using the B-H approach with wall slip levels which could be most likely reached using a coating such as a fluoroelastomer. The numerical simulations provided an explanation as to why the elongational viscosity values determined in the SHPB die for resins such as LDPE, which are extensional-strain hardening, are less sensitive to wall slip than non-strain-hardening resins such as LLDPE.

## ZUSAMMENFASSUNG:

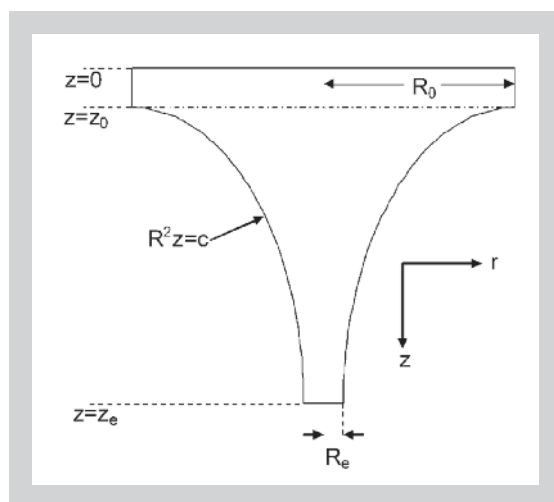
Messungen mit einer semi-hyperbolischen Düse (SHPB) mit und möglicherweise ohne Wandschmierung wurden als eine Methode vorgestellt, die Dehnviskosität von Polymerflüssigkeiten zu bestimmen. Mittels numerischer Simulationen unter der Annahme vollständigen Wandgleitens wurde für zwei Polyethylene (LDPE und LLDPE) gefunden, dass die berechnete Dehnviskosität mit denen über die Dehnung gemittelten Werten gut übereinstimmt, die unabhängig bei Messungen mit Dehnrheometern bestimmt worden sind. Dies steht im Einklang mit der Hypothese von Everage and Ballman (E-B). Numerische Simulationen zeigten, dass der Ansatz von Baird und Huang (B-H) zur Berechnung der Dehnviskosität, der die Scherspannung aufgrund des vollständigen Wandgleitens berücksichtigt, mit den experimentellen Daten besser übereinstimmt als der E-B-Ansatz. Numerische Simulationen für unterschiedliche Stärken des Wandgleitens zeigten, dass adäquate Dehnviskositätswerte mit Hilfe des B-H-Ansatzes erhalten wurden für Wandgleitenstärken, die einer Oberflächenbeschichtung aus einem Fluorelastomer entsprechen. Die numerischen Simulationen geben eine Erklärung dafür, warum die Dehnviskosität, die für LDPE mittels einer SHPB-Düse bestimmt wurde, weniger von der Stärke des Wandgleitens abhängt als für das nichtdehnverfestigende LLDPE.

## RÉSUMÉ:

La filière semi-hyperbolique (SHPB) avec ou sans effet lubrifiant aux parois a été proposée comme un appareil pour mesurer la viscosité d'élongation de fluides de polymères. En utilisant une simulation numérique avec condition de glissement total aux parois, nous avons découvert pour deux polyéthylènes (LDPE et LLDPE) que les valeurs calculées pour les viscosités d'élongation sont en bon accord avec les valeurs moyennées en déformation,  $\langle\eta_e\rangle$ , obtenues à partir de mesures indépendantes réalisées avec des rhéomètres d'étirement. Ceci concorde avec l'hypothèse originelle d'Everage et Ballman (E-B). Les simulations numériques montrent que l'approche de Baird et Huang (B-H) pour le calcul de  $\langle\eta_e\rangle$ , qui tient compte de la contrainte de cisaillement associée aux considérations géométriques en présence de glissement total, est en meilleur accord avec les données que ne l'est l'approche de E-B. Les simulations numériques avec différents degrés de glissement aux parois indiquent que des valeurs raisonnables de  $\langle\eta_e\rangle$  peuvent être obtenues en utilisant l'approche B-H avec des niveaux de glissement aux parois qui pourraient très probablement être atteints en utilisant des revêtements tels que du fluoroelastomère. Les simulations numériques fournissent une explication à la raison pour laquelle les valeurs de viscosité d'élongation déterminées dans la filière SHPB avec des résines telles que le LDPE, qui sont rhéo-durcissantes en extension, sont moins sensibles au glissement aux parois que ne le sont les valeurs obtenues pour des résines telles que les LLDPE qui ne sont pas rhéo-durcissantes.

**KEY WORDS:** numerical simulation, Phan-Thien and Tanner model, semi-hyperbolic die, extensional rheometers, strain-averaged elongational viscosity, polyethylene

Figure 1:  
Schematic of semi-hyperbolic die. Flow is from top to bottom.



## 1 INTRODUCTION

Rheologists have been looking for years for a method to determine the transient extensional viscosity,  $\eta_e^+$ , of polymer melts at high strains and strain rates. Elongational rates reached on uni-axial extensional rheometers of the Mnstedt or Meissner type are at least an order of magnitude lower than those encountered in polymer processing operations [1, 2]. Also, it is impossible to obtain accurate measurements of  $\eta_e^+$  at Hencky strains higher than about 3 for polymers that do not strain harden significantly because of sample necking.

The semi-hyperbolic (SHPB) die, as shown schematically in Figure 1, has been proposed as such a method by Collier et al. [3, 4], Everage et al. [5], James et al. [6 - 8]. With complete slip at the wall or at high Reynolds number, it has been found that in a SHPB die where the radius,  $R$ , varies according to  $R^2 z = c$ , where  $c$  is a constant determined by the geometry shown in Figure 1 and  $R$  is the radius at any  $z$ -position, there exists uni-axial extensional flow of kinematics of the form

$$\begin{aligned} v_z &= \dot{\epsilon} z \\ v_r &= -\frac{1}{2} \dot{\epsilon} r \end{aligned} \quad (1)$$

where  $v_z$  is the velocity in the flow direction,  $v_r$  is the velocity in the radial direction, and  $\dot{\epsilon}$  is the extension rate given by

$$\dot{\epsilon} = \frac{Q}{\pi R^2 z} \quad (2)$$

In Equation 2  $Q$  is the volumetric flow rate. It has been verified by James et al. [6 - 8] that a SHPB die does subject fluids to constant rates of extension in the core region of the die at high Reynolds numbers. Of course, for highly viscous polymer melts at low Reynolds numbers, lubrication is

required to eliminate the effects of shear from the die wall.

The concept of using a lubricated SHPB die to obtain extensional viscosity data was first proposed by Everage et al. [5]. A relationship between the tensile stress and the pressure drop across the lubricated die, which was corrected for the pressure drop associated with the flow of the lubricating fluid, was obtained from a force balance

$$\pi_{zz} = -\Delta P_o \quad (3)$$

where  $\pi_{zz}$  is the total stress, and the sign convention used here is that a tensile stress is negative. Everage et al. [5] recognized that the flow was unsteady in the Lagrangian sense, and, hence, they proposed that the stress values obtained from the lubricated die would provide the time or strain- averaged elongational viscosity at the strain imposed by the die. By integrating independently measured values of  $\eta_e^+$  for a polystyrene melt over the same time range as encountered in the die to obtain a time-averaged value of  $\eta_e^+$ , they reported values which they claimed were in good agreement with those obtained from the lubricated die.

More recently Collier et al. [3, 4] have revisited the use of the SHPB die to measure the elongational viscosity in the creeping flow regime, i.e. Reynolds numbers close to zero. The SHPB die was used in conjunction with a capillary rheometer and was initially fed by a polymer encapsulated with resin of much lower viscosity [3]. They demonstrated that an essentially pure elongational flow could be obtained in the core of a skin-core-coextrusion through a SHPB die where the core to skin viscosity ratio was of the order of 30 to 100 [3, 4]. Later, Collier [4] reported that it was not necessary to use lubrication as the measurements only differed within experimental error when no lubrication was used. Most of the data reported to date resemble shear viscosity data but only higher in magnitude than extensional viscosity data, which raises doubt as to the validity of the method [4].

The original analysis proposed by Collier et al. [3] was different from that of Everage et al. [5] as Collier et al. [3] assumed that the flow was steady in the Lagrangian sense, and, therefore, the extra stresses were constant throughout the

flow region. Furthermore, they, as did Everage et al. [5], neglected the contributions from  $\pi_{rz}$  (which arises as a result of the use of cylindrical coordinates to analyze a geometry that is in fact a semi-hyperbola of revolution) which was shown later by Baird et al. [9] to be negligible only at high strains. The expression obtained by Collier and coworkers by integrating the energy equation over the length of the die was supposed to yield the steady-state extensional viscosity ( $\eta_e$ , is actually referred to as the effective viscosity by Collier et al. [4]):

$$\eta_e = \frac{\Delta P_o}{\dot{\epsilon} \epsilon} \quad (4)$$

where  $\epsilon = \ln(z_e/z_o)$  is the Hencky strain with  $z_e$  and  $z_o$  defined in Figure 1,  $\dot{\epsilon}$  is the extension rate, and  $\Delta P_o$  is the pressure drop across the die. Later Feigl et al. [10] recognized that the stresses are not constant in the Lagrangian sense and suggested that at high enough Hencky strains, the stresses would reach steady state and in the presence of slip their analysis would be valid. They performed a numerical simulation of the SHPE die using a K-BKZ integral constitutive equation and reported that at Hencky strains of 6 and 7 in the presence of complete slip, numerically calculated values of extensional viscosity using the finite element method agreed with those obtained by integrating the constitutive equation over time (or strain) for a LDPE melt. Although the agreement seems quite good, it is unclear if the comparisons were always made at the same strain levels.

Baird et al. [9] made a direct comparison between values of  $\eta_e^+$  obtained by means of a Mnstedt device and the values of extensional viscosity obtained from a SHPB die without lubrication following the approach of Collier et al. [3] for three polyethylene melts. They found that the SHPB die values were significantly higher than the values obtained from the Mnstedt device. Furthermore, the values of extensional viscosity obtained from the SHPB die without lubrication were considerably higher than the strain-averaged values of extensional viscosity obtained from the Mnstedt device. They estimated the pressure drop across a SHPB die assuming resistance was all due to wall shear (using the lubrication approximation) for two polyethylene resins. In the case of LDPE the estimated values

agreed to within 20 % of the measured values suggesting that shear effects at the die wall rather than extensional stresses were dominating the pressure drop. They then presented a new analysis for extracting extensional viscosity values from pressure drop and flow rate measurements in a lubricated SHPB die, which led to the following expression for the transient normal stress difference needed to obtain the time or strain-averaged elongational viscosity at any  $z$  position (which corresponds to time or strain)

$$-(\tau_{zz} - \tau_{rr})^+ = \eta_e^+ \dot{\epsilon} = \Delta P_o - P(R) \quad (5)$$

Note that at  $z = z_e$ , the die exit,  $P(R) = 0$  and Equation 5 reduces to Equation 3, the expression proposed by Everage et al. [5]. Equation 5 shows that it may be possible to obtain  $\eta_e^+$  at any instant or strain. Based on geometric considerations and the fact that the principal stresses align with the principal strain rates in the SHPB die only at high strains, Baird et al. [9] concluded that the values of  $\eta_e^+$  (or at least the strain-averaged values) obtained from Equation 5 will be valid at Hencky strains greater than about 5.

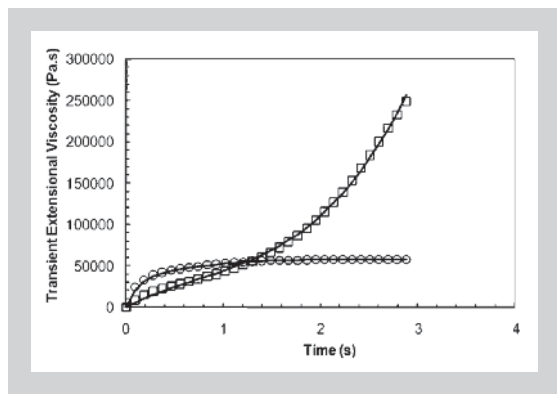
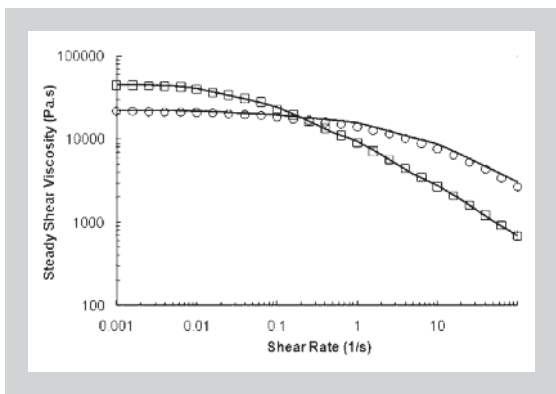
The use of the SHPB die has great potential for obtaining the extensional viscosity of polymer melts at high strains and strain rates relative to the commonly used methods involving stretching of samples with free surfaces. However, there are several issues which constitute the basis of this research and must be addressed before this method can be used to obtain reliable elongational viscosity data for polymer melts. Using numerical simulation of flow through SHPB dies and independent measurements of elongational viscosity in two different stretching devices, several key issues are addressed in this work. The first goal of this work is to determine the nature of the elongational viscosity data (is it steady, transient, or strain averaged?) obtained from the lubricated SHPB die. The second goal is to identify the theory which will give the most accurate values of elongational viscosity. The third goal is to evaluate the degree of wall slip which is needed to obtain accurate values of the elongational viscosity (must it be complete slip or just partial slip?). The final goal is to determine why certain resins yield reasonable values of elongational viscosity when measured in the SHPB die without using significant wall lubrication

Figure 2 (left): Steady shear viscosity versus shear rate at 150°C for NA952 (□) and NTX101 (○) (lines: fitted PTT).

Figure 3 (right above): Transient extensional viscosity as a function of time at an extension rate of 1 s<sup>-1</sup> and 150°C for NA952 (□) and NTX101 (○) (lines: fitted PTT).

Figure 4 (right below): Computational finite element mesh (coarse version) and flow boundaries.

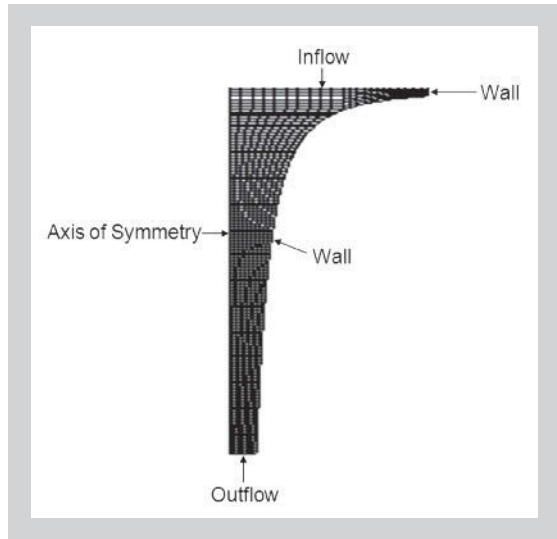
Table 1: Molecular features of two polyethylenes.



## 2 EXPERIMENTAL

The two polyethylenes considered in this study are commercially available. Their molecular characteristics are presented in Table 1. Details of the molecular characterization techniques are given elsewhere [11]. NA952 is a low-density polyethylene (LDPE) produced by Equistar Chemical. It has a high molecular weight, broad molecular weight distribution, and a high degree of short and long-chain branching. NTX101 is a linear low-density polyethylene (LLDPE) produced by Exxon-Mobil. It has a more modest molecular weight, a relatively narrow molecular distribution, and no long-chain branches.

The shear viscosity measurements for each resin were obtained from a Rheometrics Mechanical Spectrometer Model 800 (RMS-800). The shear viscosity curves for the two resins are presented in Figure 2. The dynamic oscillatory data were collected over the frequency range of 0.1 - 100 rad/s using 25 mm parallel plates. The steady shear data were collected over the shear rate range of 0.001 - 0.1 s<sup>-1</sup> using a 25 mm cone and plate fixture. The cone angle used was 0.1 radian. All testing was performed within an inert nitrogen atmosphere to prevent thermal degradation. Test samples were compression molded at 170°C and allowed to cool slowly. The results presented in Figure 2 represented an average of at least three runs using a different sample each time. High shear rate viscosity data were obtained using a Goettfert Rheograph 2001 (RG2001) capillary rheometer over the shear rate range 10 - 100 s<sup>-1</sup>. Measurements were made on three capillary dies having the same diameter of 1.0 mm but different length to diameter ratios of 10, 20, and 30. The true wall shear rate and true wall shear stress were obtained using the Rabinowitsch correction and Bagley end correction, respectively. The high shear viscosity data were

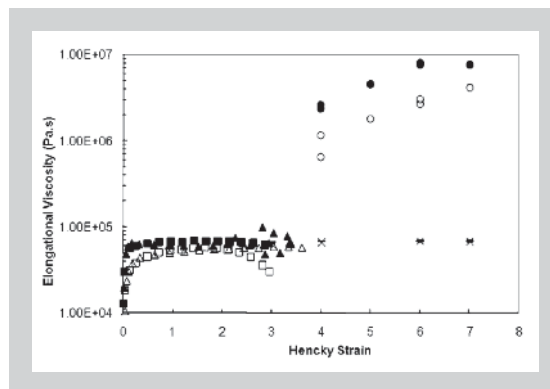
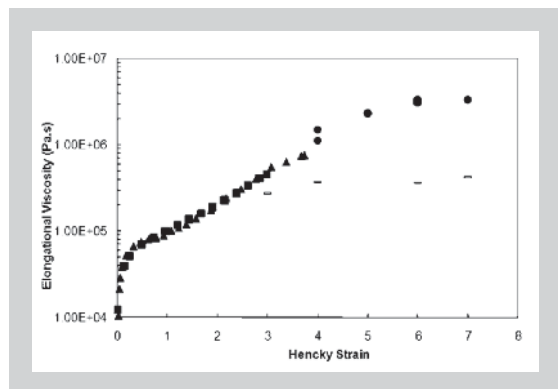


used exclusively to determine the Phan-Thien and Tanner (PTT) constitutive model parameter  $\xi$  (see below).

Uni-axial extensional stress growth measurements were obtained using a Rheometrics Extensional Rheometer Model 9000 (RER-9000) of the Mnstedt design [12]. The transient extensional data were collected over the extension rate ( $\dot{\epsilon}$ ) range of 0.01 - 1.00 s<sup>-1</sup>. The data at  $\dot{\epsilon}$  = 1.0 s<sup>-1</sup> are shown in Figure 3 for both polyethylene resins. The maximum Hencky strain achievable with this device is about 3 using test specimens with an initial nominal length of 22 mm. The cylindrical specimens were compression molded at 170°C and allowed to cool slowly. They were then bonded to test clips using high-temperature UHU<sup>®</sup> epoxy, mounted to the rheometer, and immersed in a neutrally buoyant silicone oil bath maintained at constant temperature. Once thermal equilibrium was achieved, an applied extension rate deformed the sample and the resulting force was monitored using a leaf spring - LVDT assembly. The results presented for each extension rate represent an average of at least three runs using different samples. Details of the shear and elongational viscosity measurements described above can be found elsewhere [11].

The SER testing platform developed by Sentmanat [13] is used to characterize the ex-

Resins	MFI [dg/min]	$\eta_{0, 150^{\circ}\text{C}}$ [Pa.s]	$M_w$	$M_w/M_n$	LCB/10 <sup>4</sup> C
NA952	2.0	45000	235500	17.1	39
NTX101	0.9	21 770	122700	3.44	None



tensional viscosity of a material at higher strains for extension rates of 0.1 and 1.0 s<sup>-1</sup>, and is designed to operate as a fixture in the RMS-800. A rectangular sample (8 mm width, 1.2 – 1.4 mm thickness, and 15 – 20 mm length) is placed on dual counter-rotating wind-up drums where rotation is resisted by the stretching material. The elongation rate is governed by the rotation rate and radius of the drums. The resistance to rotation force is measured by the RMS-800 torque transducer. This force is converted to the resulting transient extensional viscosity by dividing by both the applied strain rate and transient sample area. The maximum Hencky (true) strain achieved for NA952 elongated at 0.1 and 1.0 s<sup>-1</sup> was 3.73 and 3.66, respectively, and is shown in Figure 5. For NTX101, the maximum Hencky strain achieved was 3.40 and 3.61 for elongation rates of 0.1 and 1.0 s<sup>-1</sup>, respectively, and is shown in Figure 6. Material sagging was prevented by ensuring that the zero-shear viscosity at the test temperature was sufficiently high, as per the recommendation of Sentmanat [13].

Measurements were also carried out in semi-hyperbolic (SHPB) dies having an initial radius ( $R_0$ ) of 10 mm and a length ( $z_e$ ) of 25 mm (these were carried out at the University of Tennessee). Two SHPB dies, Die 1 and Die 2, were designed to provide maximum Hencky strains of 7 and 4, respectively. The dimensions of the two SHPB dies are summarized in Table 2. Data were obtained at extension rates from 0.007 to 30 s<sup>-1</sup>. The method of reducing pressure drop and flow rate data to extensional viscosity proposed by Collier et al. [3] was followed here. In essence, pressure drops and flow rates were obtained by procedures used for making measurements in a capillary rheometer. All rheological measurements were made at a temperature of 150°C

Die	$\epsilon_{\max}$	c	$R_0$ [mm]	$R_e$ [mm]	$z_0$ [mm]	$z_e$ [mm]
1	7	2.279	10	0.302	0.023	25
2	4	45.789	10	1.353	0.458	25

### 3 NUMERICAL SIMULATION

The flow problem under consideration is the viscoelastic flow through SHPB dies. We assume the flow field to be axisymmetric. For isothermal, creeping and incompressible flow, the equations of continuity and motion can be written as

$$\nabla \cdot \mathbf{v} = 0 \quad (6)$$

$$\nabla \cdot \boldsymbol{\tau} + \nabla p = 0 \quad (7)$$

where  $\nabla$  is the gradient operator,  $\mathbf{v}$  is the velocity field,  $\boldsymbol{\tau}$  is the extra stress tensor, and  $p$  is the hydrostatic pressure. The Phan-Thien and Tanner (PTT) model was chosen to describe the viscoelastic properties of the polyethylene resins utilized in this study. The PTT model is a differential constitutive equation based on network theory of concentrated polymer solutions and melts [14, 15]. A multi-mode formulation of the form below was used

$$\boldsymbol{\tau} = \sum_i \boldsymbol{\tau}_i \quad (8)$$

$$\exp\left(-\frac{\epsilon \lambda_i}{\eta_i} \text{tr} \boldsymbol{\tau}_i\right) \boldsymbol{\tau}_i + \lambda_i \tau_{i(t)} + \xi \lambda_i (\dot{\boldsymbol{\gamma}} \cdot \boldsymbol{\tau}_i + \boldsymbol{\tau}_i \cdot \dot{\boldsymbol{\gamma}}) = -\eta_i \dot{\boldsymbol{\gamma}} \quad (9)$$

where  $\dot{\boldsymbol{\gamma}}$  is the rate of deformation tensor and  $\tau_{i(t)}$  is the upper-convected derivative of stress for the  $i$ -th mode defined, respectively, by

$$\dot{\boldsymbol{\gamma}} = \nabla \mathbf{v} + \nabla \mathbf{v}^T \quad (10)$$

$$\tau_{i(t)} = \frac{\partial \boldsymbol{\tau}_i}{\partial t} + \mathbf{v} \cdot \nabla \boldsymbol{\tau}_i - (\dot{\boldsymbol{\gamma}} \cdot \boldsymbol{\tau}_i + \boldsymbol{\tau}_i \cdot \dot{\boldsymbol{\gamma}}) \quad (11)$$

The extra stress  $\boldsymbol{\tau}$  is calculated from the sum of the individual extra stresses for each mode,  $\tau_i$ ,  $\lambda_i$ , and  $\eta_i$  correspond to the relaxation time and strength for the  $i$ -th mode, respectively. In addition to the usual linear viscoelastic constants, two nonlinear parameters are also used.  $\epsilon$  characterizes the rate of destruction of entanglement “crosslinks” in the network model and has a

Figure 5 (left): Transient elongational viscosity versus Hencky strain ( $\epsilon$ ) at extension rate of 0.1 s<sup>-1</sup> for NA952. RER measured,  $\epsilon < 3$ : (■); SER measured,  $\epsilon < 4$ : (▲); SHPB die measured,  $\epsilon > 3$ , no lubrication: (●); SHPB die calculated,  $\epsilon \geq 3$ , complete wall slip: (–).

Figure 6: Transient elongational viscosity versus Hencky strain ( $\epsilon$ ) at two different extension rates  $\dot{\epsilon} = 0.1$  s<sup>-1</sup> and  $\dot{\epsilon} = 1$  s<sup>-1</sup> for NTX101. RER measured,  $\epsilon < 3$ : (■) 0.1 s<sup>-1</sup>, (□) 1 s<sup>-1</sup>; SER measured,  $\epsilon < 4$ : (▲) 0.1 s<sup>-1</sup>, (△) 1 s<sup>-1</sup>; SHPB die measured,  $\epsilon > 3$ , no lubrication: (●) 0.1 s<sup>-1</sup>, (○) 1 s<sup>-1</sup>; SHPB die calculated,  $\epsilon \geq 3$ , complete wall slip: (–) 0.1 s<sup>-1</sup>, (x) 1 s<sup>-1</sup>.

Table 2: SHPB die dimensions.



Table 3 (above):  
PTT model parameters.

Table 4:  
Numerical values of stress  
ratio  $(\tau_{zz} - \tau_{rr})/\tau_{rz}$  at the wall  
for NA952 and NTX101 in Die  
1 at  $z = 0.01$  m ( $\epsilon = 6.1$ ) under  
different wall slip condi-  
tions.

strong influence on the elongational behavior of the material, and  $\xi$  is the rate of non-affine deformation. In this study, single values of  $\epsilon$  and  $\xi$  common to all modes have been used. The above equations have been formulated using the convention described by Bird et al. [15], in which a tensile stress is taken to be negative. The boundary conditions for the flow through a SHPB die are as follows:

#### Inflow

A constant volumetric flow rate was imposed at the inflow to the die as given below

$$Q = \pi R^2 z \dot{\epsilon} = \pi c \dot{\epsilon} \quad (12)$$

where  $c$  is a constant determined by the geometry shown in Figure 1 and whose values are given in Table 2.

#### Wall

A zero normal velocity component

$$v_n = 0 \quad (13a)$$

is imposed simultaneously with a relationship between the shear force and the tangential velocity, in this case Navier's law

$$f_s = -k_{slip} v_s^{e_{slip}} \quad (13b)$$

where  $f_s$  is the tangential traction force,  $v_s$  is the tangential velocity,  $k_{slip}$  and  $e_{slip}$  are material parameters.  $k_{slip}$  was assumed to be 0,  $1 \cdot 10^6$ , and  $1 \cdot 10^9$  Pa s/m for full slip, partial slip, and no slip, respectively.  $e_{slip}$  was assumed to be 1.0 for all cases.

$\lambda_i$ [s]	$\eta_i$ (LDPE NA952) [Pa·s]	$\eta_i$ (LLDPE NTX101) [Pa·s]
0.01	$8.50 \cdot 10^2$	$3.38 \cdot 10^3$
0.1	$2.38 \cdot 10^3$	$6.36 \cdot 10^3$
1	$7.78 \cdot 10^3$	$7.37 \cdot 10^3$
10	$1.78 \cdot 10^4$	$2.89 \cdot 10^3$
100	$1.67 \cdot 10^4$	$2.09 \cdot 10^3$
$\xi$	0.191	0.179
$\epsilon$	0.034	0.239

	NA952	NTX101
Complete Slip	43.7	52.6
Partial Slip	21.0	6.2
No Slip	2.8	1.2

Note that the no slip condition,  $k_{slip} = 1 \cdot 10^9$  Pa s/m, is practically equivalent to a zero tangential velocity.

#### Axis of Symmetry

$$\begin{aligned} f_s &= 0 \\ v_n &= 0 \end{aligned} \quad (14)$$

#### Outflow

$$f_s = f_n = 0 \quad (15)$$

where  $f_n$  is the traction force in the normal direction. Note that for the flow through a SHPB die, the flow field undergoes rearrangement at the die exit, but for simplicity, boundary condition (Equation 15) was imposed. The governing equations (Equations 6–9), along with the boundary conditions (Equations 12–15), complete the mathematical description of the flow problem and were solved using POLYFLOW (Fluent Inc, version 3.10.4).

The PTT model parameters were obtained by fitting the shear and elongational viscosity data shown in Figures 2 and 3. A spectrum of five relaxation times is necessary to describe the rheological behavior of the polyethylene melts. The model parameters are summarized in Table 3. In POLYFLOW the viscoelastic predictions were determined using the elastic viscous split stress (EVSS) technique [17] coupled with inconsistent streamline upwinding (SU) [18]. This particular approach reduces the computational time and enhances the range of convergence for multi-mode viscoelastic simulations. Quadratic interpolation of the velocity field, and linear interpolation of the pressure and stress fields were utilized.

Because the governing equations for a viscoelastic fluid result in a set of highly nonlinear equations, a convergent solution cannot be obtained in a single step. The parameters leading to the nonlinearity must be incremented gradually, or evolved. In all cases for NTX101 and most cases for NA952, the volumetric flow rate,  $Q$ , was chosen as the evolution parameter. The initial flow rate was chosen such that the fluid is Newtonian in nature. Once a solution was obtained, the flow rate was gradually increased using the previous solution as an initial guess for the next evolution step. This process gradually builds the elastic contribution into the predictions. Furthermore, each intermediate solution has physical

significance because the fluid properties have not been changed, only the volumetric flow rate has. In some cases for NA952, a converged solution could not be obtained using evolution on  $Q$  alone. In such cases, the simulation began at a low flow rate, e.g.  $Q = 1 \cdot 10^{-11} \text{ m}^3/\text{s}$ , and  $\lambda_i = 0$ . The  $\lambda_i$  were gradually increased from 0 to  $\lambda_1 = 0.01 \text{ s}$ ,  $\lambda_2 = 0.1 \text{ s}$ ,  $\lambda_3 = 1 \text{ s}$ ,  $\lambda_4 = 10 \text{ s}$ , and  $\lambda_5 = 100 \text{ s}$ . Once a solution was obtained from the evolution on  $\lambda_i$ , the flow rate was gradually increased using the previous solution as an initial guess for the next step, i.e., evolution on  $Q$ . For NTX101, converged solutions were obtained up to the highest extension rate considered  $\dot{\epsilon} = 1 \text{ s}^{-1}$  ( $Q = 7.16 \cdot 10^{-9} \text{ m}^3/\text{s}$  for Die 1 and  $1.44 \cdot 10^{-7} \text{ m}^3/\text{s}$  for Die 2). For NA952, converged solutions could only be obtained up to an extension rate of about  $0.33 \text{ s}^{-1}$  ( $Q = 2.36 \cdot 10^{-9} \text{ m}^3/\text{s}$  for Die 1 and  $4.75 \cdot 10^{-8} \text{ m}^3/\text{s}$  for Die 2).

Two versions of a finite element mesh were used in the numerical simulations. The coarser and finer version contain 2040 and 20,675 elements, respectively. No significant differences were found between the simulated results obtained from the two versions. The results presented in Table 4 and Figures 5–8, 11–12, and 15–16 were obtained from the finer mesh, while the results presented in Figures 9–10, 13–14, and 17–18 were obtained from the coarser mesh. The coarser version is shown in Figure 4 together with the flow boundaries.

## 4 RESULTS AND DISCUSSION

### 4.1 SHEAR VISCOSITY

The shear viscosity data presented in Figure 2, along with the elongational viscosity data presented in Figure 3, were used to obtain the parameters of the PTT model as described above. In addition, the shear viscosity data are also important in that they provide information regarding the zero shear viscosity and a rough order of magnitude of the extensional viscosity.

### 4.2 TRANSIENT EXTENSIONAL VISCOSITY

In Figures 5 and 6 the transient extensional viscosity data obtained from the RER, SER and SHPB dies are compared for NA952 and NTX101, respectively. In each figure the transient extensional viscosity ( $\eta_e^+$ ) is plotted against the Hencky strain. For strains below 4.0, the mea-

surements were obtained from the RER and SER while for strains above 4.0 they were obtained from SHPB dies without lubrication following the method (which assumes they are the steady state values,  $\eta_e$ ) proposed by Collier et al. [3]. The calculated values of  $\eta_e^+$  based on the SHPB dies using the finite element method under full slip condition at the die wall are also presented. The calculated values at  $\epsilon = 3$  and  $\epsilon = 4$  were obtained from the Die 2 geometry while the calculated values at  $\epsilon = 6$  and  $\epsilon = 7$  were obtained from the Die 1 geometry.

In Figure 5 for NA952, only data for a single extension rate ( $\dot{\epsilon}$ ) of  $0.1 \text{ s}^{-1}$  are presented as we could not obtain converged calculated results for this material at  $1 \text{ s}^{-1}$  for making comparison with experimental results. There is good agreement between the RER and SER results at  $0.1 \text{ s}^{-1}$ , the only difference is that the SER results reach a higher Hencky strain than their RER counterparts. The RER/SER and SHPB measurements do not quite overlap, but there seems to be a trend suggesting that the two sets of data are consistent. The calculated SHPB values appear to level off (i.e. do not increase with strain) and be much lower than the measured values.

In Figure 6,  $\eta_e^+$  vs  $\epsilon$  data are presented for NTX101 at extension rates of  $0.1$  and  $1 \text{ s}^{-1}$ . Typical of a linear resin,  $\eta_e^+$  for the RER data levels off (even drops off due to necking) after  $\epsilon = 2$  for NTX101 elongated at  $1 \text{ s}^{-1}$ . The SER data pose no such problem and maintain a steady-state value up to  $\epsilon = 3.61$ . For NTX101 elongated at  $0.1 \text{ s}^{-1}$ , both the RER and SER data reach about the same steady-state value after about  $\epsilon = 1$ . However, the SER data begin to scatter after  $\epsilon = 2$ , but average out to about the same steady-state value reached earlier. The measured RER, SER and SHPB results and the calculated SHPB values all show the same qualitative trend that  $\eta_e^+$  is higher at  $0.1 \text{ s}^{-1}$  than at  $1 \text{ s}^{-1}$ . For NTX101, which does not exhibit strain hardening, but tends to reach equilibrium values of  $\eta_e^+$ , the measurements obtained from the SHPB dies without lubrication are more than an order of magnitude higher than those obtained from the RER/SER. The calculated SHPB values with full wall slip, on the other hand, are consistent with the measurements from the RER and SER.

The agreement between the numerical predictions and the experimental results for NTX101 suggests that at least with wall slip one could obtain  $\eta_e^+$  by means of the SHPB die. On the oth-

Figure 7 (left): Strain-averaged elongational viscosity versus elongation rate for NTX101. Complete wall slip condition was used in numerical simulation of flow in SHPB die. RER,  $\epsilon = 3$ : ( $\blacklozenge$ ); SHPB measured, no lubrication,  $\epsilon = 4$ : ( $\blacktriangle$ ); SHPB calculated,  $\epsilon = 3$ : ( $\times$ ); Baird & Huang,  $\epsilon = 3$ : ( $\square$ ); Everage & Ballman,  $\epsilon = 4$ : ( $\circ$ ).

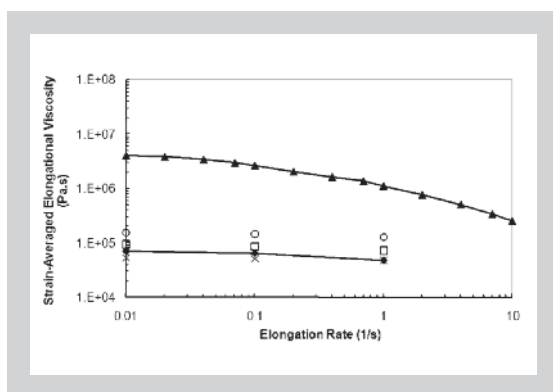
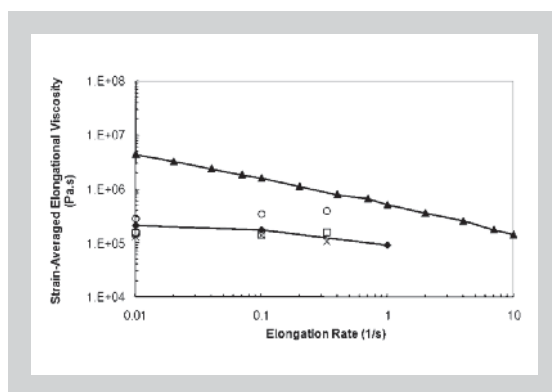


Figure 8: Strain-averaged elongational viscosity versus elongation rate for NA952. Complete wall slip condition was used in numerical simulation of flow in SHPB die. RER,  $\epsilon = 3$ : ( $\blacklozenge$ ); SHPB measured, no lubrication,  $\epsilon = 4$ : ( $\blacktriangle$ ); SHPB calculated,  $\epsilon = 3$ : ( $\times$ ); Baird & Huang,  $\epsilon = 3$ : ( $\square$ ); Everage & Ballman,  $\epsilon = 4$ : ( $\circ$ ).



er hand, there appears to be disagreement between the calculated and measured values of  $\eta_e^+$  for the LDPE sample. We do note, however, that there is only a limited range of strain where there is overlap between the calculated values and measured values of  $\eta_e^+$ . Of course, what is more puzzling is the suggested agreement between the values obtained by means of RER and SER measurements and those from the SHPB die with no lubrication shown in Figure 5 for NA952. Although it is encouraging to see that there might be agreement (again there is only a limited range of strain for overlap), we believe it occurs partly because the pressure drop associated with the extensional stress due to the strain hardening extensional viscosity significantly overrides the pressure drop due to the shear viscosity. The method (Equation 3) works, provided wall slip is present, for NTX101 and other materials in which the elongational viscosity quickly reaches a steady-state value, because for such materials the transient elongational viscosity is about the same as the strain-averaged elongational viscosity. In addition, for LDPE the predicted values of  $\eta_e^+$  based on the numerical simulation are lower than those based on Equation 3 and pressure measurements in the SHPB die which is probably due to the fact that strain averaged values of  $\eta_e^+$  are really obtained from the SHPB.

We also note that Collier and co-workers [19] suggested an orientation number to explain the agreement between techniques for some samples and lack of agreement for others. The orientation number was taken as the product of Hencky strain, elongational strain rate, and average relaxation time. When it was less than one a relaxation dominant regime results, when greater than one an orientation dominant regime results, and near one a transition occurs. For the SHPB die technique, in which the polymers are transversely constrained by the walls, the extrudates in the transition regime were believed to have slight surface defects and the pressure fluctuated more than in the other regimes. If the transition occurred after significant time, i.e., lower elongational strain rates, in

the free boundary Meissner and Instron devices, the samples apparently experienced more relaxation since unconstrained transversely (and perhaps differential thinning) leading to disagreement with the hyperbolic die measurements. The orientation related body forces were proposed to be magnitudes larger than the shearing forces and caused slip at the wall in the hyperbolic dies in the orientation dominant regime. Even in the relaxation dominant regime, shear near the wall was thought to be a minor contributor to the necessary pressure force.

#### 4.3 STRAIN-AVERAGED EXTENSIONAL VISCOSITY

Everage et al. [5] proposed that the pressure drop across a SHPB die would provide a strain-averaged extensional viscosity. Baird et al. [9] presented a new analysis for the SHPB die to determine the strain-averaged extensional viscosity from measurements of pressure at the die wall. Using the measured extensional stress growth data from the RER, the strain-averaged extensional viscosity at three extension rates was determined and is shown in Figures 7 and 8 for NTX101 and NA952, respectively. The measured values from a SHPB die without lubrication (using Equation 3), the calculated values based on the same SHPB die using the finite element method under the complete slip condition at the die wall, and the predicted values according to the expressions of Everage et al. [5] (Equation 3) and Baird et al. [9] (Equation 5) based on calculated wall pressure values from the same finite-element numerical simulation are also presented in Figures 7 and 8. All SHPB die measurements and calculations were performed on Die 2. In the legend boxes in Figures 7 and 8, the numbers in parentheses indicate the Hencky strains at which the respective strain-averaged values were determined.

Based on the results given in Figure 6, it is expected that for NTX101 the calculated strain-averaged extensional viscosity obtained from the SHPB die with complete wall slip is about the same as the measured strain-averaged extensional viscosity obtained from the RER at the



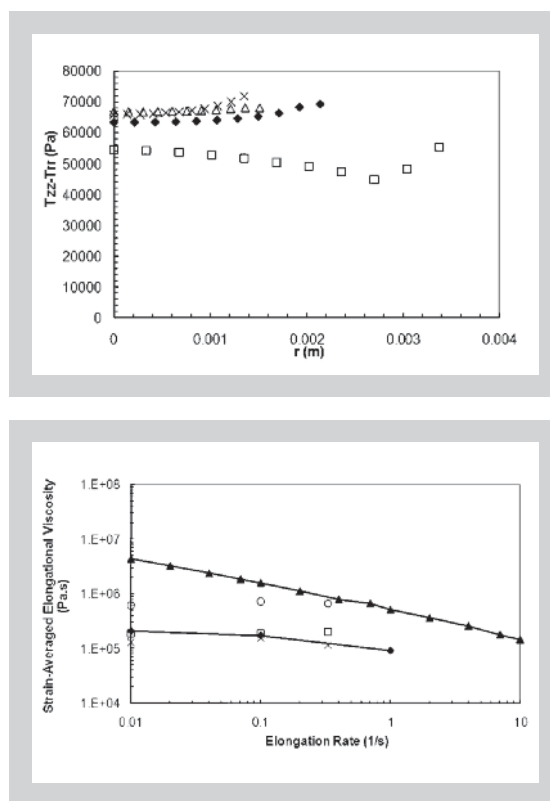
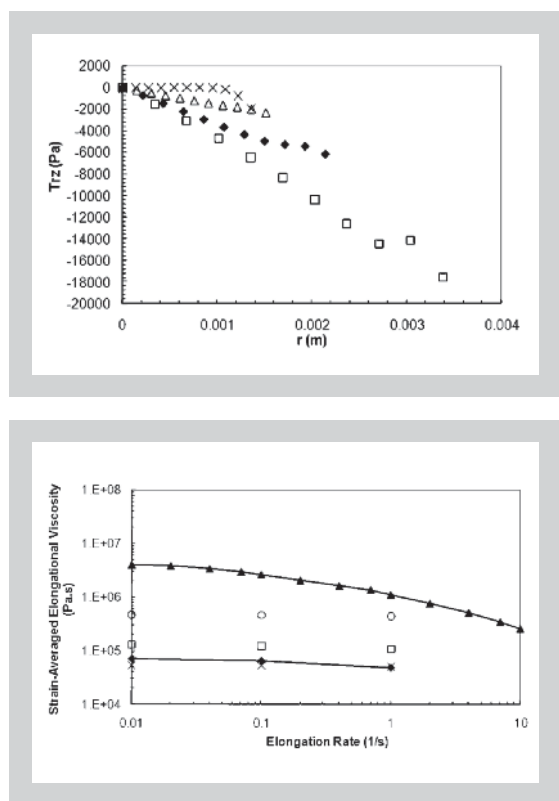


Figure 9 (left above): Calculated values of shear stress  $\tau_{rz}$  for NTX101 versus radial distance  $r$  at an extension rate of  $1 \text{ s}^{-1}$  for different axial distances  $z$  from the die entrance in a SHPB die designed to produce a maximum Hencky strain of 4 with complete wall slip.  $z = 0.004 \text{ m}$ ,  $\epsilon = 2.2$ : (□);  $z = 0.01 \text{ m}$ ,  $\epsilon = 3.1$ : (◆);  $z = 0.02 \text{ m}$ ,  $\epsilon = 3.8$ : (△);  $z = 0.025 \text{ m}$ ,  $\epsilon = 4$ : (x).

Figure 10 (right above): Calculated values of tensile stress  $\tau_{zz} - \tau_{rr}$  NTX101 versus radial distance  $r$  at an extension rate of  $1 \text{ s}^{-1}$  for different axial distances  $z$  from the die entrance in a SHPB die designed to produce a maximum Hencky strain of 4 with complete wall slip.  $z = 0.004 \text{ m}$ ,  $\epsilon = 2.2$ : (□);  $z = 0.01 \text{ m}$ ,  $\epsilon = 3.1$ : (◆);  $z = 0.02 \text{ m}$ ,  $\epsilon = 3.8$ : (△);  $z = 0.025 \text{ m}$ ,  $\epsilon = 4$ : (x).

same Hencky strain, as shown in Figure 7. This is believed to be true because the strain-averaged extensional viscosity is about the same as the transient extensional viscosity at high enough Hencky strains for a LLDPE which does not exhibit strain hardening. It is more interesting to see from Figure 8 that the calculated values from the SHPB die with complete wall slip are also close to the measured values from the RER for NA952, a LDPE that does exhibit strain hardening. This agreement reaffirms contention of Everage et al. [5] that a SHPB die with lubrication yields a strain-averaged extensional viscosity. The measured values of the strain-averaged extensional viscosity obtained from the SHPB die with no lubrication, on the other hand, are about an order of magnitude larger than the strain-averaged values from the RER, as shown in both Figure 7 and 8. This large discrepancy is unlikely to be due to the difference in Hencky strain involved (3 in the RER but 4 in the SHPB die), but rather to the absence of lubrication on the die wall. This suggests that the strain-averaged extensional viscosity cannot be obtained from the SHPB die without some degree of lubrication on the die wall (The question is: must it be complete slip or partial slip?).

The predicted values of strain-averaged extensional viscosity according to the expression of Baird et al. [9] (Equation 5) at  $\epsilon = 3$  are somewhat larger than the calculated values from the same SHPB die for both NTX101 and NA952, as shown in Figure 7 and 8, respectively. The numerical values of the normal stress difference,  $\tau_{zz} - \tau_{rr}$ ,

used to calculate the strain-averaged extensional viscosity were taken from the centerline ( $r = 0$ ) where the shear stress is zero, while the numerical values of pressure used in the expression of Baird et al. [9] (Equation 5) were taken from the die wall ( $r = R(z)$ ) where the effect of shear is at the maximum. While the shear stress,  $\tau_{rz}$ , is zero everywhere in a cylindrical die with complete slip at the wall,  $\tau_{rz}$  is not zero except at the centerline in a SHPB die under the condition of complete slip at the wall, as shown in Figure 9 for NTX101. The corresponding values of  $\tau_{zz} - \tau_{rr}$  for the same SHPB die are given in Figure 10. It can be seen that for NTX101  $\tau_{rz}$  is close to 9 % of  $\tau_{zz} - \tau_{rr}$  at the wall at a Hencky strain of 3.1 ( $z = 0.01 \text{ m}$ ) and an extension rate of  $1 \text{ s}^{-1}$ . The values predicted by the expression of Everage et al. [5] (Equation 3) at  $\epsilon = 4$  are larger than the values predicted by the expression of Baird et al. [9] simply because of the higher Hencky strain involved, as the two expressions are identical at the die exit, i.e.  $\epsilon = 4$ .

The values of strain-averaged extensional viscosity calculated from numerical results of  $\tau_{zz} - \tau_{rr}$  and predicted by numerical results of pressure under partial slip at the wall ( $k_{slip} = 1 \cdot 10^6 \text{ Pa}\cdot\text{s}/\text{m}$ ,  $e_{slip} = 1$  in Equation 13b) are given in Figures 11 and 12 for NTX101 and NA952, respectively. The calculated values based on the SHPB die with partial wall slip are still close to the measured values from the RER for both NTX101 and NA952, as the numerical results of  $\tau_{zz} - \tau_{rr}$  used to calculate the strain-averaged extensional viscosity from the SHPB die were taken from the centerline where the flow is least affected by

Figure 11 (left below): Strain-averaged elongational viscosity versus elongation rate for NTX101. Partial wall slip condition was used in numerical simulation of flow in SHPB die. RER,  $\epsilon = 3$ : (◆); SHPB measured, no lubrication,  $\epsilon = 4$ : (▲); SHPB calculated,  $\epsilon = 3$ : (x); Baird & Huang,  $\epsilon = 3$ : (□); Everage & Ballman,  $\epsilon = 4$ : (○).

Figure 12 (right below): Strain-averaged elongational viscosity versus elongation rate for NA952. Partial wall slip condition was used in numerical simulation of flow in SHPB die. RER,  $\epsilon = 3$ : (◆); SHPB measured, no lubrication,  $\epsilon = 4$ : (▲); SHPB calculated,  $\epsilon = 3$ : (x); Baird & Huang,  $\epsilon = 3$ : (□); Everage & Ballman,  $\epsilon = 4$ : (○).

Figure 13 (left):  
Calculated values of shear stress  $\tau_{rz}$  NTX101 versus radial distance  $r$  at an extension rate of  $1 \text{ s}^{-1}$  for different axial distances  $z$  from the die entrance in a SHPB die designed to produce a maximum Hencky strain of 4 with partial wall slip.  
 $z = 0.004 \text{ m}$ ,  $\epsilon = 2.2$ : ( $\square$ );  
 $z = 0.01 \text{ m}$ ,  $\epsilon = 3.1$ : ( $\blacklozenge$ );  
 $z = 0.02 \text{ m}$ ,  $\epsilon = 3.8$ : ( $\triangle$ );  
 $z = 0.025 \text{ m}$ ,  $\epsilon = 4$ : ( $\times$ ).

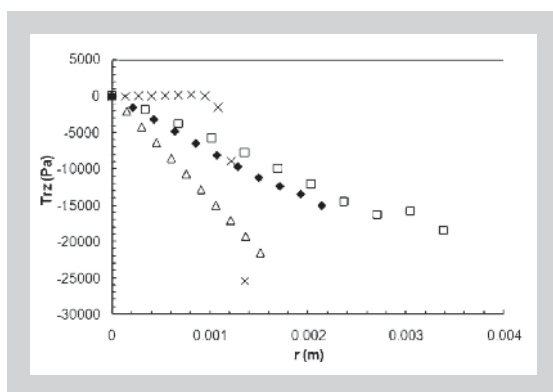
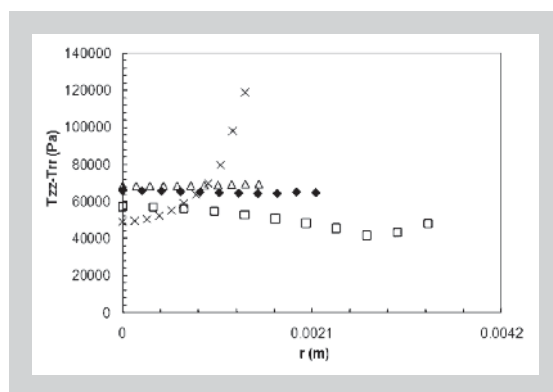


Figure 14:  
Calculated values of tensile stress  $\tau_{zz} - \tau_{rr}$  NTX101 versus radial distance  $r$  at an extension rate of  $1 \text{ s}^{-1}$  for different axial distances  $z$  from the die entrance in a SHPB die designed to produce a maximum Hencky strain of 4 with partial wall slip.  
 $z = 0.004 \text{ m}$ ,  $\epsilon = 2.2$ : ( $\square$ );  
 $z = 0.01 \text{ m}$ ,  $\epsilon = 3.1$ : ( $\blacklozenge$ );  
 $z = 0.02 \text{ m}$ ,  $\epsilon = 3.8$ : ( $\triangle$ );  
 $z = 0.025 \text{ m}$ ,  $\epsilon = 4$ : ( $\times$ ).



shear. The difference between the strain-averaged extensional viscosity calculated from  $\tau_{zz} - \tau_{rr}$  and that predicted by the expression of Baird et al. [9] has become larger with some frictional force at the die wall than the case with complete wall slip, but the values are closer to what is expected than predicted by the method of Everage et al. [5]. For NTX101 under the above condition of partial slip at the wall, the calculated value of  $\pi_{rz}$  is about 23% of  $\pi_{zz} - \pi_{rr}$  at the die wall at a Hencky strain of 3.1 ( $z = 0.01 \text{ m}$ ) and an extension rate of  $1 \text{ s}^{-1}$ , according to the numerical results shown in Figures 13 and 14. In other words, there is some contribution to the pressure drop from the resistance to flow at the die wall. However, with a reasonable level of slip, which seems feasible using a coating such as polytetrafluoroethylene (PTFE), it appears to be possible to obtain strain-averaged values of extensional viscosity using the SHPB and Equation 5.

The values of strain-averaged extensional viscosity calculated from numerical results for  $\tau_{zz} - \tau_{rr}$  and predicted by numerical results for pressure drop with no slip at the wall are given in Figures 15 and 16 for NTX101 and NA952, respectively. The calculated values from the SHPB die with no wall slip are somewhat larger than the measured values from the RER for both NTX101 and NA952, even though the numerical results of  $\tau_{zz} - \tau_{rr}$  used in the calculations were taken from the centerline where the flow should be least affected by shear. The difference between the strain-averaged extensional viscosity calculated from  $\tau_{zz} - \tau_{rr}$  and that predicted by the expression of Baird et al. [1] (Equation 5) has become very large with no slip at the die wall as the pressure drop is now dominated by shear at the die wall. In Figures 17 and 18 it is shown that under the condition of no slip at the wall, the calculated value of  $\pi_{rz}$  is about as large as  $\pi_{zz} - \pi_{rr}$  at the wall for NTX101 at a Hencky strain of 3.1 ( $z = 0.01 \text{ m}$ ) and an extension rate of  $1 \text{ s}^{-1}$ . For both NA952 and NTX101, the values predicted by the expressions of Everage et al. [5] (Equation 3) and Baird et al. [9] (Equation 5) are of the same order of magnitude as the measured values obtained from the SHPB die with no lubrication, reaffirming that the large discrepan-

cy between the measured values from the SHPB die with no lubrication and those from the RER is not due to the slight difference in Hencky strain involved but to the absence of lubrication on the wall of the SHPB die. This discrepancy is smaller for NA952, which exhibits strain hardening, than for NTX101, which does not strain harden, consistent with the higher tensile stress relative to the shear stress for a strain-hardening material such as NA952. The values of the ratio of calculated  $\tau_{zz} - \tau_{rr}$  to calculated  $\tau_{rz}$  (stress ratio) for NA952 and NTX101 are compared in Table 4 under the conditions of full slip, partial slip and no slip at the wall. It is obvious from Table 4 that the effect of shear stress is less important for NA952 than for NTX101, except in the case of full slip at the wall, where the stress ratio is large for both NA952 and NTX101. This calculation and associated observation somewhat confirm the earlier explanation of the data presented in Figures 5 and 6 in which there appeared to be agreement between the transient extensional viscosity measured in the RER or SER and that obtained in a SHPB die for LDPE but not for LLDPE.

## 5 CONCLUSIONS

The overall goal of this work has been to provide a better understanding of the conditions under which one can obtain elongational viscosity values for polymer melts from the SHPB die and the nature of the values obtained from this device. Numerical simulations of flow in SHPB dies under conditions of perfect wall slip showed that the strain-averaged elongational viscosity rather than the steady-state elongational viscosity is obtained from a SHPB die confirming the original hypothesis of Everage et al. [5]. This result is based on comparing calculated values of extensional viscosity from tensile stresses taken at the centerline of a SHPB die to those measured independently in stretching rheometers, the SER and RER, and strain-averaged. The analysis of Baird et al. [9], which is an extension of the work of Everage et al. [5], provides a method for extracting the strain-averaged viscosity from wall pressure measurements in the SHPB die which appears to yield values which agree better with the values

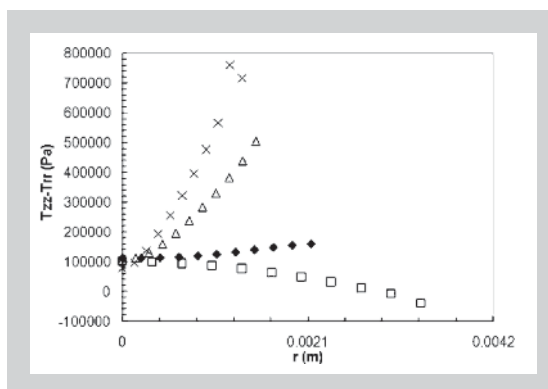
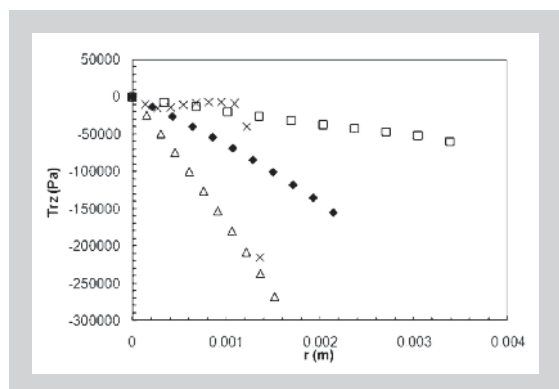
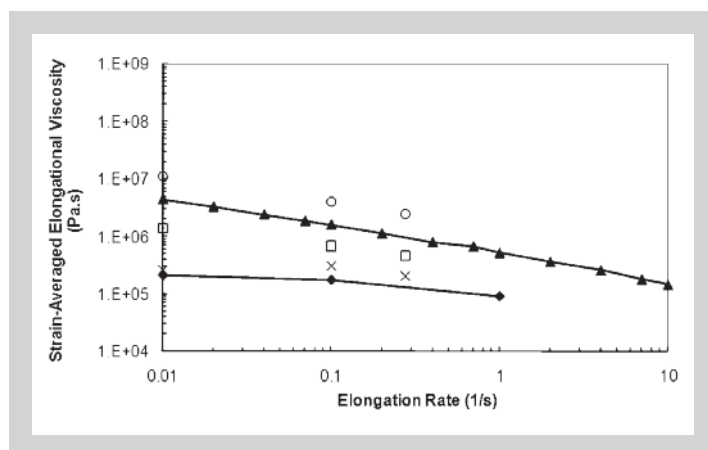
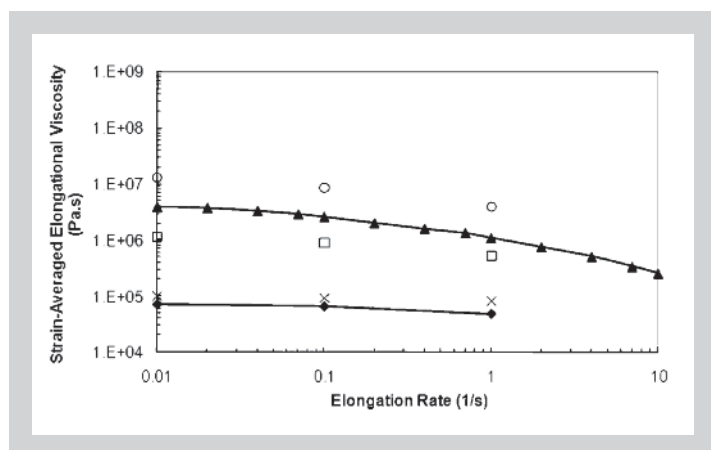


Figure 15 (left above): Strain-averaged elongational viscosity versus elongation rate for NTX101. No wall slip condition was used in numerical simulation of flow in SHPB die. RER,  $\epsilon = 3$ : (♦); SHPB measured, no lubrication,  $\epsilon = 4$ : (▲); SHPB calculated,  $\epsilon = 3$ : (x); Baird & Huang,  $\epsilon = 3$ : (□); Everage & Ballman,  $\epsilon = 4$ : (○).

Figure 16 (right above): Strain-averaged elongational viscosity versus elongation rate for NA952. No wall slip condition was used in numerical simulation of flow in SHPB die. RER,  $\epsilon = 3$ : (♦); SHPB measured, no lubrication,  $\epsilon = 4$ : (▲); SHPB calculated,  $\epsilon = 3$ : (x); Baird & Huang,  $\epsilon = 3$ : (□); Everage & Ballman,  $\epsilon = 4$ : (○).

measured in the RER and SER than do the values obtained from the method of Everage et al. For both LDPE and LLDPE, the predictions of Baird et al. [9] agree with measurements from the RER and SER provided there is a sufficient degree of slip at the wall, but perfect slip does not seem to be required based on the numerical simulations. In fact, it is proposed that a surface coating applied to the die walls such as a fluoroelastomer could provide sufficient slip. With increasing wall resistance to the flow, the effect of shear stress on wall pressure measurements becomes increasingly dominant, making the predictions of Baird et al. [9] too high but approaching those determined from the SHPB die and the method proposed by Collier and coworkers. The effect of shear stress on the elongational viscosity measurements in a SHPB die is smaller for LDPE which exhibits extensional strain-hardening than for LLDPE which does not exhibit strain-hardening.

## ACKNOWLEDGEMENT

This research was part of a collaborative effort under the World Wide Network of Materials and the support provided by the National Science Foundation under grant number DMR-052198 is greatly appreciated.

## REFERENCES

- [1] Barnes HA, Hutton JF, Walters K: An Introduction to Rheology, Elsevier Amsterdam (1989).
- [2] Filipe S, Becker A, Barroso VC, Wilhelm M: Evalu-

- ation of melt flow instabilities of high-density polyethylenes via an optimised method for detection and analysis of the pressure fluctuations in capillary rheometry, Appl. Rheol. 19 (2009) 23345.
- [3] Collier JR, Romanoschi O, Petrovan S: Elongational rheology of polymer melts and solutions, J. App. Polym. Sci. 69 (1998) 2357-2367.
- [4] Collier JR: Elongational rheometer and on-line process controller, US Patent 6,220,083 (2001).
- [5] Everage AE, Ballman RL: The extensional flow capillary as a new method for extensional viscosity measurement, Nature 273 (1978) 213-215.
- [6] James DF, Chandler GM, Armour SJ: A converging channel rheometer for the measurement of extensional viscosity, J. Non-Newt. Fluid Mech. 35 (1990) 421-443.
- [7] James DF, Chandler GM, Armour SJ: Measurement of the extensional viscosity of M1 in a converging channel rheometer, J. Non-Newt. Fluid Mech. 35 (1990) 445-458.
- [8] James DF: Flow in a converging channel at moderate Reynolds number, AIChE J. 37-1 (1991) 59-64.
- [9] Baird DG, Huang J: Elongational viscosity measurements using a semi-hyperbolic die, Appl. Rheol. 16 (2007) 312-320.
- [10] Feigl K, Tanner FX, Edwards BJ, Collier JR: A numerical study of the measurement of elongational viscosity of polymeric fluids in a semihyperbolically converging die, J. Non-Newt. Fluid Mech. 115 (2003) 191-215.
- [11] Doerpinghaus PJ, Baird DG: Assessing the branching architecture of sparsely branched metallocene-catalyzed polyethylenes using the Pom-Pom constitutive model, Macromolecules 35 (2002) 10087-10095.

Figure 17 (left below): Calculated values of shear stress  $\tau_{rz}$  versus radial distance,  $r$ , for NTX101 at an extension rate of  $1 \text{ s}^{-1}$  for different axial distances  $z$  from the die entrance in a SHPB die designed to produce a maximum Hencky strain of 4 with no wall slip.  $z = 0.004 \text{ m}$ ,  $\epsilon = 2.2$ : (□);  $z = 0.01 \text{ m}$ ,  $\epsilon = 3.1$ : (♦);  $z = 0.02 \text{ m}$ ,  $\epsilon = 3.8$ : (Δ);  $z = 0.025 \text{ m}$ ,  $\epsilon = 4$ : (x).

Figure 18 (right below): Calculated values of tensile stress  $\tau_{zz} - \tau_{rr}$  versus radial distance,  $r$ , for NTX101 at an extension rate of  $1 \text{ s}^{-1}$  for different axial distances  $z$  from the die entrance in a SHPB die designed to produce a maximum Hencky strain of 4 with no wall slip.  $z = 0.004 \text{ m}$ ,  $\epsilon = 2.2$ : (□);  $z = 0.01 \text{ m}$ ,  $\epsilon = 3.1$ : (♦);  $z = 0.02 \text{ m}$ ,  $\epsilon = 3.8$ : (Δ);  $z = 0.025 \text{ m}$ ,  $\epsilon = 4$ : (x).

- [12] Münstedt, H: New universal extensional rheometer for polymer melts. Measurements on a polystyrene sample, *J. Rheol.* 23 (1979) 421-436.
- [13] Sentmanat ML: Miniature universal testing platform: from extensional rheology to solid-state deformation behavior, *Rheol. Acta* 43 (2004) 657-669.
- [14] Phan-Thien N, Tanner RI: A new constitutive equation derived from network theory, *J. Non-Newt. Fluid Mech.* 2 (1977) 353-365.
- [15] Phan-Thien N: A nonlinear network viscoelastic model, *J. Rheol.* 22 (1978) 259.
- [16] Bird RB, Armstrong RC, Hassager O: Dynamics of Polymeric Liquids Vol. 1 Fluid Mechanics, John Wiley & Sons, New York (1987). [17]
- Rajagopalan D, Armstrong RC, Brown RA: Calculation of steady viscoelastic flow using a multimode Maxwell model: application of the explicitly elliptic momentum equation (EEME) formulation, *J. Non-Newt. Fluid Mech.* 36, (1990) 135-137.
- [18] Marchal JM, Crochet MJ: A new mixed finite element for calculating viscoelastic flow, *J. Non-Newt. Fluid Mech.* 26 (1987) 77-114.
- [19] Collier JR, Petrovan S, Hudson N, Wei X: Elongational rheology by different methods and orientation number, *J. App. Polym. Sci.* 105 (2007) 3551-3561.

